The Astrophysical Journal, 662: L35–L38, 2007 June 10

INTERACTION BETWEEN A FAST ROTATING SUNSPOT AND EPHEMERAL REGIONS AS THE ORIGIN OF THE MAJOR SOLAR EVENT ON 2006 DECEMBER 13

Jun Zhang, Leping Li, and Qiao Song
National Astronomical Observatories, Chinese Academy of Sciences, Beijing 100012, China; zjun@ourstar.bao.ac.cn, lepingli@ourstar.bao.ac.cn, qiaosong@ourstar.bao.ac.cn
Received 2007 March 28; accepted 2007 April 30; published 2007 May 23

ABSTRACT

The major solar event on 2006 December 13 is characterized by the approximately simultaneous occurrence of a heap of hot ejecta, a great two-ribbon flare, and an extended Earth-directed coronal mass ejection. We examine the magnetic field and sunspot evolution in NOAA AR 10930, the source region of the event, while it transited the solar disk center from December 10 to 13. We find that the obvious changes in the active region associated with the event are the development of magnetic shear, the appearance of ephemeral regions, and fast rotation of a smaller sunspot. Around the area of the magnetic neutral line of the active region, interaction between the fast rotating sunspot and the ephemeral regions triggers continual brightening and finally the major flare. This indicates that only after the sunspot rotates up to 200° does the major event take place. The sunspot rotates at least 240° about its center, the largest sunspot rotation angle that has been reported.

Subject headings: Sun: activity — Sun: atmospheric motions — Sun: flares — Sun: magnetic fields

1. INTRODUCTION

Solar flares are powered by the energy stored in the stressed magnetic field; strong flares tend to occur in the vicinity of magnetic neutral lines where the field gradients are strong and the horizontal components are highly sheared (e.g., Harvey & Harvey 1976; Wang et al. 1994, 2002; Deng et al. 2006). The movement of magnetic footpoints by photospheric flows can lead to the destabilization of the magnetic field and hence to flares by increasing the length of the field lines in the corona (e.g., Somov et al. 2002). On the other hand, Nindos & Zhang (2002) have pointed out that shearing motions have little effect in the process of buildup of magnetic free energy that leads to the initiation of coronal mass ejections (CMEs).

Observations indicate that reconnection-favored emerging flux has a strong correlation with flare onset and CMEs (Schmieder et al. 1997; Ishii et al. 1998; Kusano et al. 2002; Kurokawa et al. 2002; Sakajiri et al. 2004). Based on the flux rope model, an emerging flux trigger mechanism is proposed for the onset of CMEs, using two-dimensional magnetohydrodynamic (MHD) numerical simulations (Chen & Shibata 2000).

Besides magnetic field observations in active regions, white-light observations furthermore have shown sunspot evolution, for example, sunspot rotation (Evershed 1910; Maltby 1964; Gopasyuk 1965). Stenflo (1969) has suggested that sunspot rotation may be involved with energy buildup and later release by a flare. With the high spatial and temporal resolution of recent satellite-borne telescopes, the observations of rotating sunspots and other magnetic structures have become more frequent and easier to identify (Nightingale et al. 2000, 2002; Brown et al. 2001). The sigmoid structures (Canfield & Pevtsov 1999), which are thought to be more likely to erupt and cause flares and CMEs, may be associated with the rotation of the magnetic footpoints in the photosphere. Brown et al. (2003) have shown that some sunspots rotate up to 200° about their umbral center, and the corresponding loops in the coronal fan twist and erupt as flares.

The major event on 2006 December 13 exhibits almost simultaneous plasma ejecta, flare activity, and a CME. It provides a good opportunity to study the surface magnetic activity and sunspot kinematics that result in the rather global magnetic instability. In this Letter, we examine the magnetic evolution and sunspot rotation prior to and during the course of the major event with the emphasis on the interaction of a rotating sunspot and ephemeral regions that characterizes this CME-producing active region.

2. OBSERVATIONS

NOAA AR 10930 displayed the evolution of a complex magnetic structure, surrounded by many small dark pores and bright magnetic faculae, as observed by the the *Solar and Heliospheric Observatory* (*SOHO*) Michelson Doppler Imager (MDI; Scherrer et al. 1995) and the *Transition Region and Coronal Explorer* (*TRACE*; Handy et al. 1999) over a 12 day interval from 2006 December 6 to December 18. The data set analyzed consists of 4 day (from December 10 to 13) full-disk magnetograms obtained from MDI, synchronous high-resolution white light, and UV (1600 Å) observations from the *TRACE* satellite, with spatial resolution of 1.0″, temporal resolution of 20–60 s, and field of view of 384″ × 384″. Figure 1 shows the general appearance of NOAA AR 10930 in the decaying phase of the major flare.

3. RESULTS OF OBSERVATIONS

By checking the MDI and *TRACE* data, we note that the first obvious magnetic evolution in NOAA AR 10930 is the developing of magnetic shear. Figure 2 presents the time sequence of the MDI longitudinal magnetograms (*left*), the corresponding *TRACE* continuum images (*middle*), and the corresponding *TRACE* 1600 Å images (*right*). Two contours in the continuum images at December 10 12:50 and 22:30 UT outline a dark thread, which connects the pair of opposite polarity sunspots of the active region. These contours are overplotted onto the corresponding longitudinal magnetograms and *TRACE* 1600 Å images. Before December 10, 12:51 UT, the thread connects directly with the two sunspots. Ten hours later, although the thread still joins the two sunspots, its shape changes from beeline to reverse S-shaped curve. Gradually, the thread disappears and some new threads appear along the neutral line of the two sunspots (see Fig. 2, *dashed curves on*

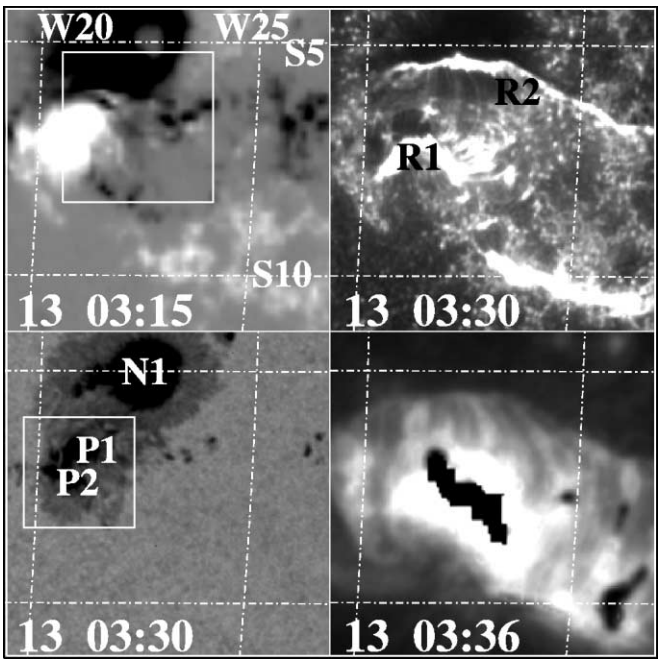

FIG. 1.—General appearance of NOAA AR 10930 at different wavelengths in the decaying phase of the major flare. *Upper left*: MDI longitudinal magnetogram. The window outlines a subarea where ephemeral regions appear (see Fig. 4). *Lower left*: Corresponding continuum intensity image from *TRACE*. N1 is the main sunspot of the active region; P1 and P2 are the following sunspots. The window denotes the field of view of Fig. 5, where the sunspot P1 fast rotates;. *Upper right*: Corresponding *TRACE* 1600 Å image showing the two ribbons (R1 and R2) of the flare. *Lower right*: Corresponding *TRACE* 195 Å image showing the postflare loops. The dash-dotted lines represent the solar latitudes and longitudes. The field of view is about 120″ × 120″.

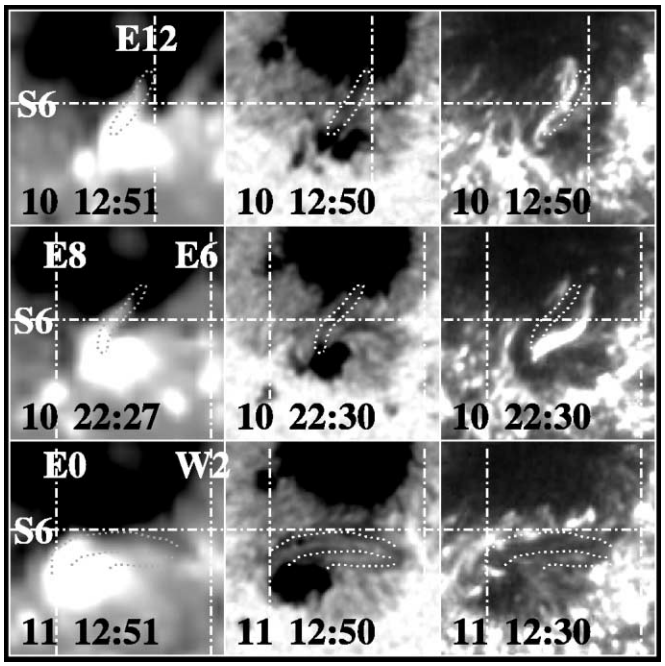

FIG. 2.—Time sequence of the MDI longitudinal magnetograms (*left column*), the corresponding *TRACE* continuum images (*middle column*), and the corresponding *TRACE* 1600 Å images (*right column*), showing the developing of magnetic shear. The field of view is about 50″ × 50″. The dotted contours and curves are described in the text.

the continuum image in the bottom panel). From the MDI magnetogram on December 11 at 12:51 UT, we find that these new threads seem to be arch filament systems connecting the opposite polarities of ephemeral regions (ERs) that emerge along the neutral line of AR 10930. Figure 3 clearly shows an ER (*two pairs of arrows*) on high-resolution MDI magnetograms, while the magnetic shear of the active region is well developed. First, the two magnetic elements belonging to the ER are ellipses in shape and separate each other with a speed of 0.5 km s^{-1}. After 4 hr evolution, the shape of the elements looks like two narrow ribbons along the neutral line of the active region, as the ER is squeezed tightly by the region. In the process of the ER appearing, multiple neutral lines (Fig. 3, *top right panel*, *dark lines*) develop, and continuous UV brightening appears in the area of these neutral lines.

We have noted that ERs appear not only prior to the onset of the major solar event but also during the course of the event. Figure 4 shows an ER appearing during the flare/CME event. The arrows point to the ER. The positive element of the ER plunges into the neutral line area of the active region. Before it merges to the positive polarity magnetic field of the active region, it cancels with surrounding opposite polarity field; meanwhile UV brightening appears. The bright material ejects along the axis of the ER to the right (shown by the arrow in the *TRACE* 1600 Å image at 01:40 UT). Twenty minutes later, the major flare takes place. The negative element moves away from the active region with a speed of 0.5 km s^{-1}. At 06:05 UT, the distance between the two elements is about 22,000 km, and a UV bright ribbon connects with the two elements of the ER.

Observations from *TRACE* in the photospheric white-light channel have shown that from the end of December 10 on, sunspot rotation in the active region accompanies the magnetic flux emergence in the form of ERs in the neutral line area. Figure 5 shows an example of the rotation of a dark penumbral feature "f3" (*arrows*). The feature first appeared near December 12, 00:10 UT, it rotated around the center (*circles*) of the smaller spot. From December 12, 00:10–20:50 UT, the dark feature rotated about 190°,

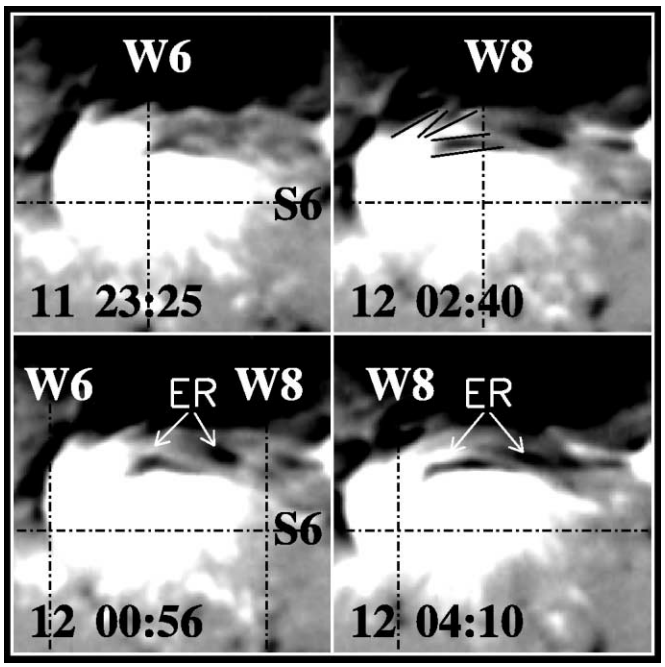

FIG. 3.—Time sequence of high-resolution MDI longitudinal magnetograms, showing emergence flux that appears near the magnetic neutral line of the active region, after the AR 10930 magnetic shear is well developed. The field of view is about 60″ × 60″. The arrows and the dark lines are described in the text.

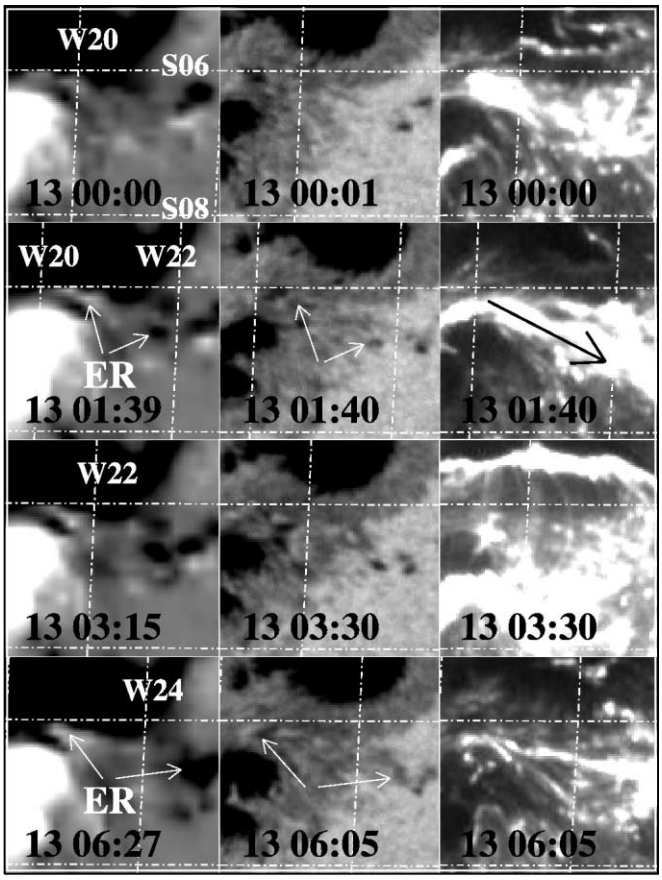

FIG. 4.—Time sequence of MDI longitudinal magnetograms (*left column*), the corresponding *TRACE* continuum images (*middle column*), and the corresponding *TRACE* 1600 Å images (*right column*), showing the appearance of bipolar magnetic features during the course of the major flare/CME event. The field of view is about 50″ × 50″. The arrows are described in the text.

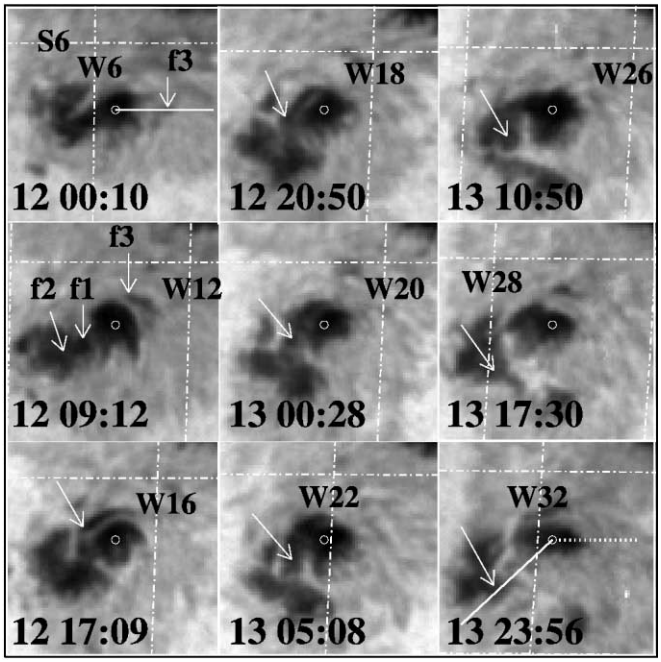

FIG. 5.—Time sequence of *TRACE* continuum images showing the rotation of a dark penumbral feature (f3) around the center (*circles*) of P1 mentioned in Fig. 1. f1 and f2 are other two rotating dark features which appear prior to the emergence of f3. The three arrows in the continuum image at December 12, 09:12 UT point to the three features (f1, f2, and f3), otherwise the arrows points to f3. The convergence of f1, f2, and other unresolved features forms P2 (see Fig. 1). The two solid lines in the first and last images connect f3 with the center of gravity of P1, and the dotted line in the last image is a duplicate of the solid line in the first image. The field of view is about 40″ × 40″.

and the mean angular speed reaches 9° hr^{-1}. In the following 14 hr, the feature became larger and larger, due to the converging of other unresolved features. The angular speed decreased to 2° hr^{-1} on average. Finally, the dark feature broke up and gradually decayed. By checking the continuum data, we can clearly identify that in the penumbra of the smaller sunspot, there are several dark features that rotated around the spot. Figure 6 shows the rotation of the three penumbral features mentioned in Figure 5. It shows that a penumbral feature started to rotate while the shear developed, and the rotational speed is about 20° hr^{-1}. Between 02:00 and 12:00 UT on December 12, the rotational speed of all three features is low with a mean value of 4° hr^{-1}. Several hours prior to the flaring activity, all three features underwent a fast rotational process (Fig. 6, *bottom panel*, *circles*). Before the flare took place, the rotational angle of each feature exceeded 200°. During the course of the flaring activity, these features displayed a relatively low rotational speed. After the onset of the flaring activity, these features continuously rotated around the sunspot with a mean speed of 2° hr^{-1}. Near the end of December 13, the amount of the rotational angle for each feature was around 240°. This is the largest angle that has been reported.

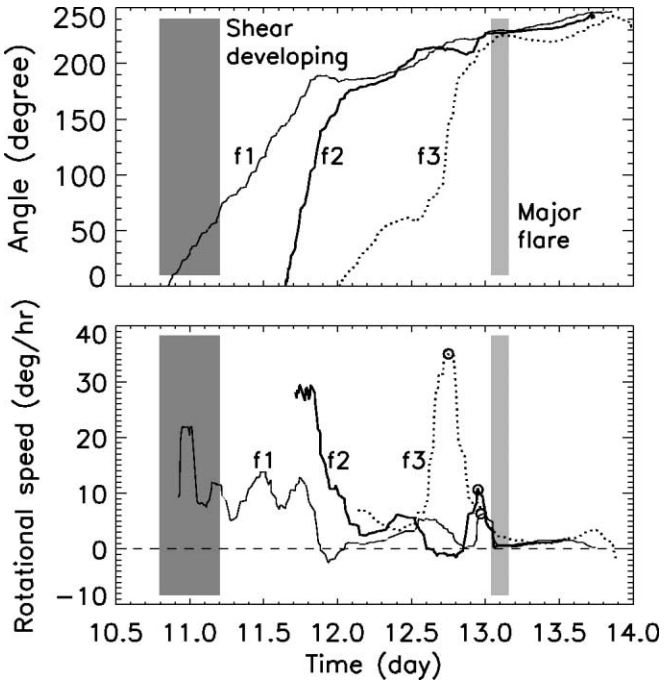

FIG. 6.—Plots showing rotational angle (*top*) of the three penumbral features (f1, f2, and f3 shown in Fig. 5) and rotational speed (*bottom*) of the corresponding features vs. time. Dark gray area represents the shear developing period and the light gray area the flaring activity period. The minus rotational speed of these features corresponds to the stage when the features move away from the sunspot. Three circles in the bottom panel are described in the text.

4. DISCUSSION AND CONCLUSIONS

It is commonly accepted that a solar flare suddenly releases magnetic free energy that is stored in the form of a stressed magnetic topology (e.g., Deng et al. 2006). Magnetic flux emergence and cancellation may play an important role in injecting

magnetic energy through the photosphere into the corona. Wang & Shi (1993) presented a two-step reconnection scenario for flare process. The first step of reconnection is seen as flux cancellation observed in the photosphere (Zhang et al. 2001). This reconnection first stores the magnetic energy necessary for flares (Somov 2006) and then transports the energy into the coronal magnetic structure. The second step of reconnection is directly responsible for transient solar activities and takes place only when some critical status is achieved in the corona.

Motions of the photospheric sources lead to buildup of current layers parallel to a separator that separates the interacting magnetic fluxes (Sweet 1969; Lau 1993; see Somov 2006 for a review). Régnier & Canfield (2006) have identified that in NOAA AR 8210, a fast motion of an emerging polarity is associated with small-scale reconnections, and a sunspot rotation enables the occurrence of flare by a reconnection process close to a magnetic surface. Gerrard et al. (2003) have simulated the rotation of a pore around a sunspot. While the pore rotates 180° around the sunspot, the current increases rapidly as the center of the pore makes contact with the large sunspot. This current buildup could be an explanation of an observed flaring. Observations (see, e.g., Fig. 6) are consistent with the simulation of Gerrard et al.

In this study, the major solar event manifests itself as bright plasma ejecta, a great flare, and an extended Earth-directed CME. For such a major event, the obvious activities in its source region are the development of magnetic shear, the appearance of ephemeral regions, and fast rotation of a sunspot. More importantly, the major event takes place only after the rotational angle of the sunspot reached 200°. It is prefigurative that the interaction between ephemeral regions and fast rotation of a sunspot plays a decisive role in producing the global instability responsible for this major solar event.

We are keenly conscious of the limitations imposed by the low spatial resolution of MDI magnetograms. Higher spatial resolution is likely to uncover the nature of the source regions of major solar events. A detailed study of this flare/CME event is planned with *Hinode* data.

The authors are indebted to the *TRACE* and *SOHO* MDI teams for providing the data. *SOHO* is a project of international cooperation between ESA and NASA. This work is supported by the National Natural Science Foundations of China (G10573025, 10603008, and 40674081), the CAS Project KJCX2-YW-T04, and the National Basic Research Program of China under grant G2006CB806303.

REFERENCES

Brown, D. S., Nightingale, R. W., Alexander, D., Schrijver, C. J., Metcalf, T. R., Shine, R. A., Title, A. M., & Wolfson, C. J. 2003, Sol. Phys., 216, 79
Brown, D. S., Parnell, C. E., Deluca, E. E., Golub, L., & McMullen, R. A. 2001, Sol. Phys., 201, 305
Canfield, R. C., & Pevtsov, A. A. 1999, in Magnetic Helicity in Space and Laboratory Plasmas, ed. M. R. Brown, R. C. Canfield, & A. A. Pevtsov (Geophys. Monogr. 111; Washington, DC: AGU), 197
Chen, P. F., & Shibata, K. 2000, ApJ, 545, 524
Deng, N., Xu, Y., Yang, G., Cao, W., Liu, C., Rimmele, T. R., Wang, H., & Denker, C. 2006, ApJ, 644, 1278
Evershed, J. 1910, MNRAS, 70, 217
Gerrard, C. L., Brown, D. S., Mellor, C., Arber, T. D., & Hood, A. W. 2003, Sol. Phys., 213, 39
Gopasyuk, S. I. 1965, Izv. Krymskoi Astrofiz. Obs.. 33, 100
Handy, B. N., et al. 1999, Sol. Phys., 187, 229
Harvey, K. L., & Harvey, J. W. 1976, Sol. Phys., 47, 233
Ishii, T. T., Kurokawa, H., & Takeuchi, T. T. 1998, ApJ, 499, 898
Kurokawa, H., Wang, T., & Ishii, T. T. 2002, ApJ, 572, 598
Kusano, K., Maeshiro, T., Yokoyama, T., & Sakurai, T. 2002, ApJ, 577, 501
Lau, Y. T. 1993, Sol. Phys., 148, 301
Maltby, P. 1964, Astrophys. Norvegica, 8, 205
Nightingale, R. W., et al. 2000, Eos Trans. AGU, 81, Fall Meeting Suppl., No. SH11A-10
———. 2002, in *Yohkoh* 10th Anniv. Meeting: Multi-Wavelength Observations of Coronal Structure and Dynamics, ed. P. C. H. Martens & D. Cauffman (New York: Elsevier), 149
Nindos, A., & Zhang, H. 2002, ApJ, 573, L133
Régnier, S., & Canfield, R. C. 2006, A&A, 451, 319
Sakajiri, T., et al. 2004, ApJ, 616, 578
Scherrer, P. H., et al. 1995, Sol. Phys., 162, 129
Schmieder, B., Aulanier, G., Démoulin, P., van Driel-Gesztelyi, L., Roudier, T., Nitta, N., & Cauzzi, G. 1997, A&A, 325, 1213
Somov, B. V. 2006, Plasma Astrophysics, Part II: Reconnection and Flares (New York: Springer)
Somov, B. V., Kosugi, T., Hudson, H. S., & Sakao, T. 2002, ApJ, 579, 863
Stenflo, J. O. 1969, Sol. Phys., 8, 115
Sweet, P. A. 1969, ARA&A, 7, 149
Wang, H., Ewell, M. W., Zirin, H., & Ai, G. 1994, ApJ, 424, 436
Wang, H., Spirock, T. J., Qiu, J., Ji, H., Yurchyshyn, V., Moon, Y.-J., Denker, C., & Goode, P. R. 2002, ApJ, 576, 497
Wang, J., & Shi, Z. 1993, Sol. Phys., 143, 119
Zhang, J., Wang, J., Deng, Y., & Wu, D. 2001, ApJ, 548, L99